

Spectral function of a hole in the t - J model

Zhiping Liu and Efstratios Manousakis

Department of Physics, Center for Materials Research and Technology and Supercomputer Computations Research Institute, Florida State University, Tallahassee, Florida 32306

(Received 16 April 1991)

We give numerical solutions, on finite but large-size square lattices, of the equation for the single-hole Green's function obtained by the self-consistent approach of Schmitt-Rink *et al.* and Kane *et al.* The spectral function of the hole in a quantum antiferromagnet shows that most features describing the hole motion are in close agreement with the results of the exact diagonalization on the 4^2 lattice in the region of $J/t \leq 0.2$. Our results obtained on sufficiently large-size lattices suggest that certain important features of the spectral function survive in the thermodynamic limit while others change due to finite-size effects. We find that the leading nonzero vertex correction is given by a two-loop diagram, which has a small contribution.

It has been suggested¹ that the basic physics of the copper oxide planes of high-temperature superconductors may be described by a two-dimensional (2D) single-band Hubbard model. In the strong-coupling limit and at half filling this model reduces to the spin- $\frac{1}{2}$ antiferromagnetic Heisenberg model. The effect of doping is to remove electrons thereby producing mobile holes in the CuO_2 planes. For small doping, the motion of holes in a Heisenberg antiferromagnet can be described by the following model:

$$\hat{H}_{t-J} = -t \sum_{(i,j),\sigma} (c_{i\sigma}^\dagger c_{j\sigma} + \text{H.c.}) + J \sum_{(i,j)} \mathbf{S}_i \cdot \mathbf{S}_j, \quad (1)$$

where $c_{i,\sigma}$ is a hole creation operator and t the electron hopping matrix element. The strong on-site Coulomb repulsion is taken into account by restricting the action of the Hamiltonian operator in a subspace of the Hilbert space having states with singly occupied sites. The Hamiltonian (1), now known as the " t - J model," has received significant attention by various authors because it can be derived from more realistic models that account for the detailed chemical structure of the copper oxide planes.² It combines an antiferromagnetic exchange known to account for many of the magnetic properties of the undoped insulating cuprous oxides³ that become superconductors upon doping and a hopping matrix element to describe hole conductivity.

Many attempts have been made to study the 2D t - J model in the presence of a single hole, using both analytical and numerical techniques. Green's-function techniques,^{4,5} variational approaches,⁶⁻⁸ and exact diagonalization studies⁹⁻¹¹ as well as other studies¹² have provided useful information about certain features of the single-hole dispersion relation and the spectral function.

In this paper we present numerical solutions for the Dyson's equation of a single-hole Green's function in the t - J model on a square lattice using the approach of Schmitt-Rink *et al.*⁴ and Kane *et al.*⁵ We compare the hole spectral function with the exact results obtained on a 4^2 lattice by Dagotto *et al.*⁹ and find that they are in

very close agreement in the small- J region. The results on larger-size lattices confirm the existence of string excitations above the quasiparticle peak and suggest that the pseudogap,⁹ which exists on a 4^2 lattice, may be due to the finite-size effects. Furthermore, we find that the one-loop diagram of vertex correction is zero so that the leading nonzero vertex correction to the hole Green's function is given by a two-loop diagram that has a small contribution. Our numerical results on the hole spectrum have been obtained without the additional dominant-pole approximation used by Kane *et al.*, therefore this work provides complementary information based on the method developed in Refs. 4 and 5.

Following the work of Schmitt-Rink *et al.*, we write the hopping Hamiltonian as

$$H_t = t \sum_{(i,j)} [(1 - b_i^\dagger b_i) h_i^\dagger b_j^\dagger h_j + h_i^\dagger h_j b_i (1 - b_j^\dagger b_j)] + \text{H.c.}, \quad (2)$$

where h_i^\dagger is a spinless fermion operator that creates holes and b_i^\dagger is a hard-core boson operator. We define $h_i = c_{i\uparrow}^\dagger$ and $b_i^\dagger = S_i^-$ on the \uparrow sublattice and $h_i = c_{i\downarrow}^\dagger$ and $b_i^\dagger = S_i^+$ on the \downarrow sublattice. In the linear spin-wave approximation one keeps terms only up to quadratic in the hard-core boson operators in both the Heisenberg and hopping terms of Eq. (1) and diagonalizes the J term using the standard approach of spin-wave theory for antiferromagnets, namely by means of a Bogoliubov transformation. In this approximation the term (2) couples the holes to the spin waves as

$$H_t \simeq tz N^{-1/2} \sum_{\mathbf{k},\mathbf{q}} h_{\mathbf{k}-\mathbf{q}}^\dagger [\alpha_{\mathbf{q}} (u_{\mathbf{q}} \gamma_{\mathbf{k}-\mathbf{q}} + v_{\mathbf{q}} \gamma_{\mathbf{k}}) + \alpha_{-\mathbf{q}}^\dagger (v_{\mathbf{q}} \gamma_{\mathbf{k}-\mathbf{q}} + u_{\mathbf{q}} \gamma_{\mathbf{k}})] + \text{H.c.}, \quad (3)$$

where N is the total number of sites and

$$u_{\mathbf{k}} = [(1 - \gamma_{\mathbf{k}}^2)^{-1/2} + 1]^{1/2} / \sqrt{2}, \quad (4)$$

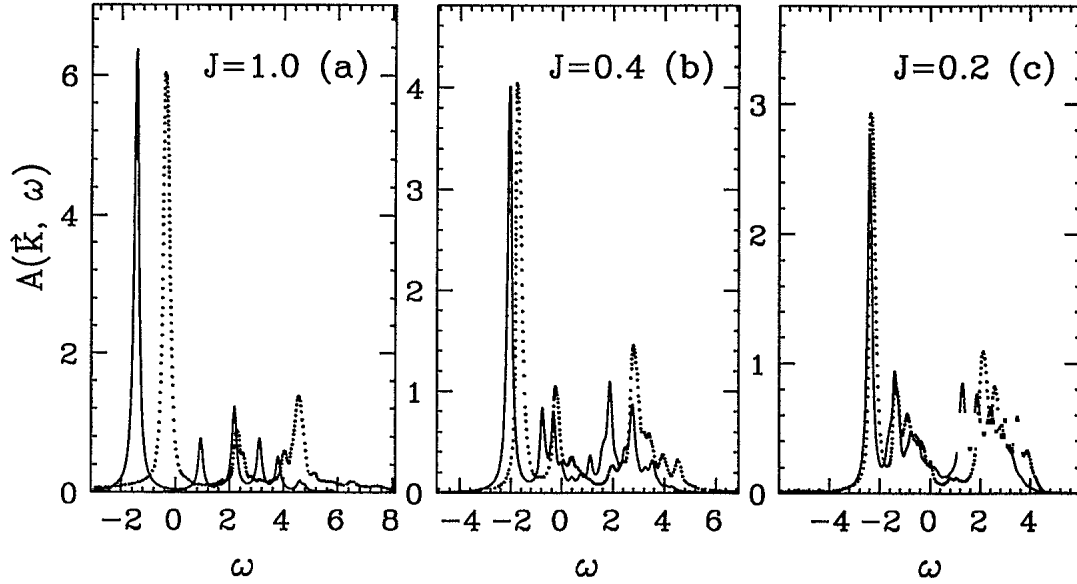


FIG. 1. $A(\mathbf{k}, \omega)$ with $\mathbf{k} = (\pi/2, \pi/2)$ calculated on a 4^2 lattice for typical values of J using $\epsilon = 0.1$. The dotted lines correspond to those shown in Fig. 5 of the paper by Dagotto *et al.* (Ref. 9) The spectral function is normalized according to our definition of $A(\mathbf{k}, \omega)$. Note that the agreement is good for small values of J , while for large J the locations of the peaks are at significantly different energies.

$$v_{\mathbf{k}} = -\text{sgn}(\gamma_{\mathbf{k}})[(1 - \gamma_{\mathbf{k}}^2)^{-1/2} - 1]^{1/2}/\sqrt{2}, \quad (5)$$

and $\gamma_{\mathbf{k}} = \sum_{\delta} e^{i\mathbf{k}\cdot\delta}/z$, and z is the number of the nearest neighbors. The α 's are spin-wave operators related to the b 's via the Bogoliubov transformation $b_{\mathbf{k}} = u_{\mathbf{k}}\alpha_{\mathbf{k}} + v_{\mathbf{k}}\alpha_{-\mathbf{k}}^{\dagger}$ with dispersion $\Omega_{\mathbf{q}} = JzS\sqrt{1 - \gamma_{\mathbf{q}}^2}$.

In the limit $J \ll t$, using a self-consistent perturbation approach where only noncrossing diagrams are summed, one obtains the following expression for the hole propagator:

$$G(\mathbf{k}, \omega) = \frac{1}{\omega - \sum_{\mathbf{q}} f^2(\mathbf{k}, \mathbf{q})G(\mathbf{k} - \mathbf{q}, \omega - \Omega_{\mathbf{q}})}, \quad (6)$$

where

$$f(\mathbf{k}, \mathbf{q}) \equiv zt(\gamma_{\mathbf{k}-\mathbf{q}}u_{\mathbf{q}} + \gamma_{\mathbf{k}}v_{\mathbf{q}})/\sqrt{N}. \quad (7)$$

Equation (6) has been numerically solved in one-dimension (1D) by Schmitt-Rink *et al.*⁴ The 2D case has been extensively studied analytically by Kane *et al.*⁵ in the various limits. They used the so-called dominant-pole approximation, which assumes that the hole spectrum is incoherent above the quasiparticle peak. In this paper, we give the numerical solutions obtained by iterating Eq. (6) on finite clusters of size $N = L \times L$ starting from

$$G^{(0)}(\mathbf{k}, \omega) = \frac{1}{\omega + i\epsilon}. \quad (8)$$

We have assumed that the output of the n th iteration $G^{(n)}(\mathbf{k}, \omega)$ has both real and imaginary parts $G^{(n)}(\mathbf{k}, \omega) = G_R^{(n)}(\mathbf{k}, \omega) + iG_I^{(n)}(\mathbf{k}, \omega)$, where $G_R^{(n)}(\mathbf{k}, \omega)$

and $G_I^{(n)}(\mathbf{k}, \omega)$ are the results of the n th iterations of coupled equations derived from Eq. (6). The spectral function $A(\mathbf{k}, \omega) = -(1/\pi)G_I^{(\infty)}(\mathbf{k}, \omega)$ is obtained after the convergence for a given lattice size and given value of ϵ is achieved.

First, we would like to compare our results to those obtained by means of exact diagonalization on the 4^2 size lattice for the single-hole case. We set $t = 1$. In Fig. 1, we compare our results (the solid lines) of $A(\mathbf{k}, \omega)$ calculated on a 4^2 lattice for typical values of J with Fig. 5 of the paper by Dagotto *et al.*⁹ (the dotted lines) using the same value of ϵ . The agreement is good for small values of J , while for large values of J the locations of the peaks are at significantly different energies. We also calculate the energies of the lowest-energy peaks on the 4^2 lattice for different values of J 's and \mathbf{k} 's. We find that the states \mathbf{k} and $\mathbf{k} - (\pi, \pi)$ are always degenerate in our calculation, which is not true in the exact diagonalization study. For the 4^2 lattice, the hole ground state is a degenerate state with momenta $\mathbf{k} = (\pi/2, \pi/2)$, $(\pi, 0)$, and $(0, \pi)$. The same degeneracy also exists in the exact hole ground state.⁹ On the other hand, the minimum of the hole band in the present method corresponds to $\mathbf{k} = (\pi/2, \pi/2)$ for the sizes of lattices larger than 4^2 . The energy band has very similar features to those found by other calculations,¹² namely, an anisotropic effective mass with a large value in the direction $(\pi, 0)$ to $(0, \pi)$ of the Brillouin zone and a small mass in the orthogonal direction.

In Table I, we compare the energies and the residues of the lowest-energy peaks for different J 's with exact results. We also give the results on a 16^2 lattice where finite-size effects are negligible. The quasiparticle en-

TABLE I. The energy at $\mathbf{k} = (\pi/2, \pi/2)$ and the residue of the quasiparticle peak on a 4^2 lattice are compared to the results obtained by exact diagonalization (numbers in the parentheses) to test the range of validity of the present method. We also give the results on a 16^2 lattice where finite-size effects are negligible. The value of $\epsilon = 0.1$ has been used.

J	E (4×4)	E (16×16)	a (4×4)	a (16×16)
0.10	-2.640(-2.643)	-2.778	0.230(0.20)	0.247
0.20	-2.388(-2.298)	-2.544	0.296(0.28)	0.277
0.30	-2.208(-1.997)	-2.364	0.362(0.35)	0.322
0.40	-2.058(-1.722)	-2.214	0.414(0.40)	0.367
0.55	-1.872(-1.344)	-2.022	0.485(0.46)	0.427
0.70	-1.712(-0.993)	-1.860	0.543(0.51)	0.477
1.00	-1.448(-0.345)	-1.590	0.642(0.59)	0.575

ergy at $\mathbf{k} = (\pi/2, \pi/2)$ can be fit with a power law as $-3.04 + 1.92J^{0.66}$ on a 4^2 lattice, and $-3.20 + 1.936J^{0.66}$ on a 16^2 lattice for the region of $0.1 \leq J \leq 0.4$. The energy deviates from the exact data on a 4^2 lattice for the values of J greater than 0.2 whereas the residues from the two calculations remain close. The residues have been calculated in our approach using $a_{\mathbf{k}} = 1/[1 - (\partial/\partial\omega)\text{Re}\Sigma]$, where the real part of the self-energy $\text{Re}\Sigma$ is evaluated at $\omega_{\mathbf{k}}$, which is the position of the quasiparticle peak. The residue of the pole at $\mathbf{k} = (\pi/2, \pi/2)$ can be fit to a form $a_{\mathbf{k}} \sim J^{0.5}$ (for $0 < J/t < 1$) which is in very good agreement with the results of Dagotto *et al.*⁹

Having shown that this method gives results in good agreement with the exact ones for the 4^2 lattice in the small- J region, we now calculate $A(\mathbf{k}, \omega)$ for larger-size lattices inaccessible to exact diagonalizations. One needs to take the limit $N \rightarrow \infty$ first and then the limit $\epsilon \rightarrow 0$; thus, we choose a value of ϵ small compared to both physical scales in the model, i.e., $\epsilon \ll J$ and $\epsilon \ll t$, but larger than the resolution $\Delta\omega = 0.006$, and we change the size of the system until we remove the finite-size effects. In

Fig. 2(a)-2(d) we show $A(\mathbf{k}, \omega)$ at $\mathbf{k} = (\pi/2, \pi/2)$ for $J = 0.1$ obtained on 4^2 , 8^2 , 16^2 , and 32^2 lattices, respectively. We have selected a small value of $\epsilon = 0.01$, which is smaller by at least an order of magnitude than both J and t . Note that only states close to the low-

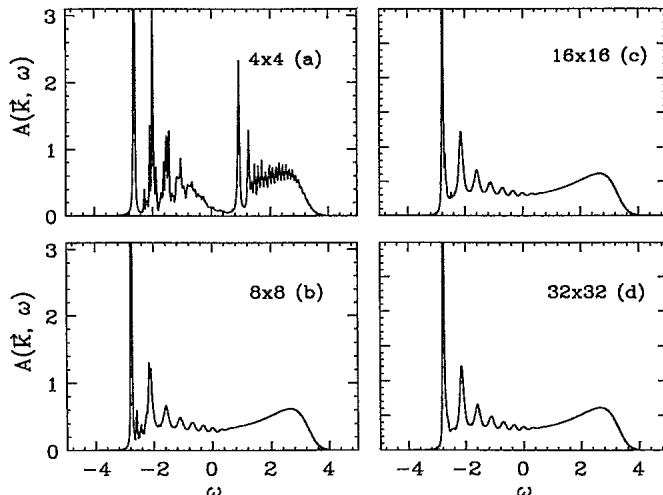
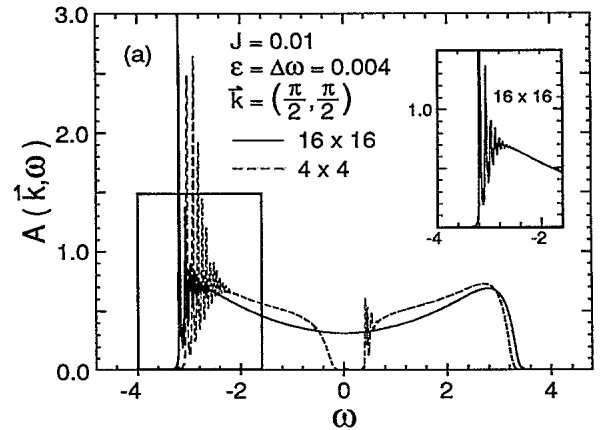


FIG. 2. $A(\mathbf{k}, \omega)$ with $\mathbf{k} = (\pi/2, \pi/2)$ for $J = 0.1$ and $\epsilon = 0.01$. The results are obtained on 4^2 , 8^2 , 16^2 , and 32^2 lattices.

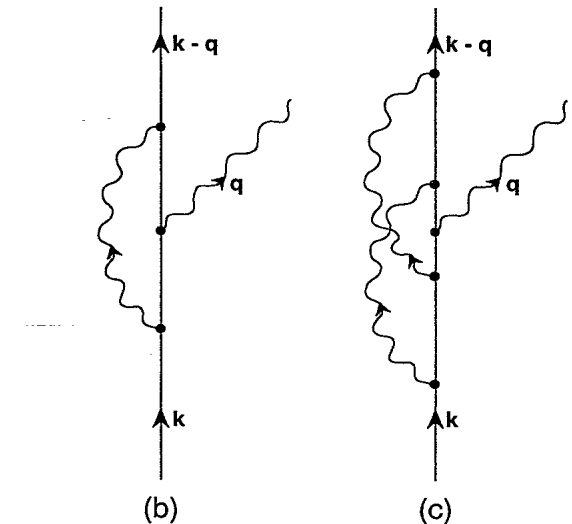


FIG. 3. (a) $A(\mathbf{k}, \omega)$ with $\mathbf{k} = (\pi/2, \pi/2)$, $\epsilon = \Delta\omega = 0.004$, and $J = 0.01$. The dotted and solid lines denote the results on 4^2 and 16^2 lattices, respectively. (b) The leading vertex correction is zero. The wavy line denotes a spin-wave propagator while the solid line denotes the hole propagator. (c) The leading nonzero vertex correction, which involves two loops.

est peak, which is the strongest (and corresponds to the quasiparticle excitation), are sensitive to the size of the lattice, for lattices larger than 8^2 . We find that there is a series of peaks above the lowest-energy peak whose intensities decrease with increasing energy. These peaks are not due to finite-size effects, they do not change by decreasing or increasing ϵ by an order of magnitude. These peaks were also found in the exact calculation on the 4^2 lattice by Dagotto *et al.*⁹ They found that the J dependence of the positions of the second-lowest-energy peak is given by $-3.13 + 5.36J^{0.70}$. Our calculation for the same size lattice gives $-2.75 + 5.49J^{0.87}$, while on a 16^2 lattice the peak is given by $-3.266 + 5.794J^{0.72}$ in the region of $0.1 \leq J \leq 0.4$. We believe that these peaks correspond to the hole excitations moving in an approximate linear potential imposed by the antiferromagnetically ordered background as predicted by Shraiman and Siggia⁶ for the t - J_z model, where these excitations have no width while in the t - J model they acquire width due to spin fluctuations. These string states need to be taken into account in the definition of the quasihole state in order to obtain an accurate description of quasiparticle operators.^{11,13}

It is worthwhile to mention that the pseudogap located for the values of ω between 0 and 2 in Fig. 1(c) and the following positive frequency peaks found in the exact diagonalization also appear in our calculation for a 4^2 lattice (see the solid line). However, we believe that these features are due to the spurious finite-size effects, because they do not show up in the larger-size lattices, as shown in Fig. 2(d). The spectral function in the small- J limit is shown in Fig. 3(a) for 4^2 and 16^2 lattices. In this limit the time scale for spin fluctuations is much larger than that for hole hopping, so the width of the peaks that correspond to stringlike excitations is very small. Again, the pseudogap that appeared on the 4^2 lattice

disappears on the 16^2 lattice. The first pole for the 16^2 lattice is located at $\omega_0 = -3.18$, which is close to the result obtained by setting $J = 0$ in the form $-3.17 + 2.83J^{0.73}$, which was found by Dagotto *et al.*⁹

The vertex correction diagrams containing the one shown in Fig. 3(b) do not contribute to the Green's function. This is so because $f(\mathbf{k}, \mathbf{q})$ changes sign under the transformation $\mathbf{k} \rightarrow \mathbf{k} \pm (\pi, \pi)$ or $\mathbf{q} \rightarrow \mathbf{q} \pm (\pi, \pi)$. Thus the leading nonzero vertex correction is shown in Fig. 3(c) and it involves two loops. Next, we give a crude argument which justifies the apparent success of this approximation. The dressed Green's function is of order $1/t$ (as shown by Kane *et al.*,⁵ the residue of the quasiparticle peak is of order J/t while the bandwidth of the quasiparticle state is of order J) and the vertices are of order t . Since the number of additional vertices and the number of internal hole Green's functions are the same, this diagram at first sight is of order 1. If we examine the diagram more closely, we find that each loop contributes $1/z$, z is the number of nearest neighbors, therefore the order of this two-loop diagram is $1/z^2$. Thus, we expect the vertex corrections to give a small contribution; this explains the remarkable agreement with the exact results at small J/t . At large J/t , however, the linearization of the original Hamiltonian is no longer a good approximation, in particular the hopping part cannot be correctly described by (3).

Note added in proof. After this manuscript was submitted, a paper by Marsiglio *et al.* appeared¹⁴ where a similar calculation has been performed.

This work was supported in part by the Supercomputer Computations Research Institute, which is partially funded by the U.S. Department of Energy under Contract No. DE-FC05-85ER-250000.

-
- ¹P. W. Anderson, *Science* **235**, 1196 (1987).
²F. C. Zhang and T. M. Rice, *Phys. Rev. B* **37**, 3759 (1988).
³E. Manousakis, *Rev. Mod. Phys.* **63**, 1 (1991).
⁴S. Schmitt-Rink, C. M. Varma, and A. E. Ruckenstein, *Phys. Rev. Lett.* **60**, 2793 (1988).
⁵C. Kane, P. Lee, and N. Read, *Phys. Rev. B* **39**, 6880 (1989).
⁶B. Shraiman and E. Siggia, *Phys. Rev. Lett.* **60**, 740 (1988); **61**, 467 (1988); V. Elser, D. Huse, B. Shraiman, and E. Siggia, *Phys. Rev. B* **41**, 6715 (1990).
⁷S. Sachdev, *Phys. Rev. B* **39**, 12 232 (1989); M. Boninsegni and E. Manousakis, *ibid.* **43**, 10 353 (1991).
⁸S. A. Trugman, *Phys. Rev. B* **41**, 892 (1990).
⁹E. Dagotto *et al.*, *Phys. Rev. B* **41**, 9049 (1990).
¹⁰K. J. von Szczepanski, P. Horsch, W. Stephan, and M. Ziegler, *Phys. Rev. B* **41**, 2017 (1990).
¹¹E. Dagotto and J. R. Schrieffer, *Phys. Rev. B* **43**, 8705 (1991).
¹²B. Chakraborty *et al.*, *Phys. Rev. B* **42**, 4819 (1990); S. A. Trugman, *ibid.* **37**, 1597 (1988); F. Nori, E. Abrahams, and G. Zimanyi, *ibid.* **41**, 7277 (1990); R. Shankar, *Phys. Rev. Lett.* **63**, 203 (1989); D. Poilblanc and E. Dagotto, *Phys. Rev. B* **42**, 4861 (1990); Z. Zou and R. B. Laughlin, *ibid.* **42**, 4073 (1990); J. M. F. Gunn and B. D. Simons, *ibid.* **42**, 4370 (1990); T. Itoh *et al.*, *ibid.* **42**, 4834 (1990); J. R. Schrieffer, X. G. Wen, and S. C. Zhang, *ibid.* **39**, 11 663 (1989); S. A. Trugman, *Phys. Rev. Lett.* **65**, 500 (1990).
¹³M. Boninsegni and E. Manousakis (unpublished).
¹⁴F. Marsiglio, A. E. Ruckenstein, S. Schmitt-Rink, and C. M. Varma, *Phys. Rev. B* **43**, 10 882 (1991).